Clinical and Experimental Gastroenterology

Dovepress
Taylor & Francis Group

Open Access Full Text Article

ORIGINAL RESEARCH

Network Pharmacology, Molecular Docking and Dynamics Simulation Reveal the Anti-Colitis Mechanism of *Smilax glabra* Roxb.

Yuan Cui[1,2], Jingyi Hu[1], Yanan Li[1], Yiheng Tong[1], Hong Shen[1]

[1]Department of Gastroenterology, Jiangsu Province Hospital of Chinese Medicine, Affiliated Hospital of Nanjing University of Chinese Medicine, Nanjing, 210001, People's Republic of China; [2]Department of Gastroenterology, Ningxian Second People's Hospital, Qingyang, 745200, People's Republic of China

Correspondence: Hong Shen, Department of Gastroenterology, Jiangsu Province Hospital of Chinese Medicine, Affiliated Hospital of Nanjing University of Chinese Medicine, 155 Hanzhong Road, Qinhuai District, Nanjing City, Jiangsu Province, 210001, People's Republic of China, Tel/Fax +86-025-86617141, Email shenhong999@njucm.edu.cn

Clinical and Experimental Gastroenterology downloaded from https://www.dovepress.com/
For personal use only.

Purpose: A combination of bioinformatics methods including network pharmacology, molecular docking and molecular dynamics simulation was utilized to investigate the potential mechanism of *Smilax glabra* Roxb. (SG) in the treatment of ulcerative colitis (UC).

Methods: We firstly used network pharmacology to screen out the major active components, targets and pathways. Secondly, the top 5 ingredients and the top 5 targets were docked with molecular docking technology respectively. Thirdly, the two protein-compound complexes with the lowest binding scores were subjected to molecular dynamics simulation (MDs).

Results: A total of 15 bioactive compounds and 191 targets were identified, with the top 5 compounds being quercetin, beta-sitosterol, naringenin, stigmasterol and diosgenin, and the top 5 targets being AKT1, IL-6, TNF, TP53 and IL-1β. Predominant enrichment was observed in the PI3K-Akt signaling pathway, TNF signaling pathway, IL-17 signaling pathway, MAPK signaling pathway and apoptosis. Each set of molecular docking calculations was run 50 times and repeated 3 times for statistical analysis, with results showing that the majority of binding energies were less than −5 kcal/mol, indicating successful docking. Specifically, stigmasterol–TP53 (−9.10 ± 0.07 kcal/mol) and diosgenin–TP53 (−8.80 ± 0.73 kcal/mol) are the two complexes with the lowest binding energies for MDs. According to the MDs, the stig-masterol-TP53 and diosgenin-TP53 complex shows ideal conformational stability and interaction energy.

Conclusion: Multiple components of SG may exert therapeutic effects on UC through multiple targets and various signaling pathways. Novelty of this study lies in linking SG compounds to UC-specific targets and confirming stable docking/MDs interactions with TP53. However, further validation through in vivo and in vitro experiments is required to provide reliable evidence for clinical application.

Keywords: *Smilax glabra* Roxb., ulcerative colitis, network pharmacology, molecular docking, molecular dynamics simulation

Introduction

Ulcerative colitis (UC) and Crohn's disease are the two main forms of inflammatory bowel disease (IBD).[1] Unlike Crohn's disease, UC, a chronic inflammatory disease of the intestinal mucosa, has few complications and can be cured by colectomy.[2] Although the pathophysiology of UC needs to be further explored, current studies have shown that it is mainly related to epithelial barrier, commensal microflora, antigen recognition, dysregulation of immunological responses and leucocyte recruitment.[1] In recent years, treatment goals for UC have evolved to optimize patient quality of life, including maintenance of steroid-free remission, prevention of hospitalization and surgery, mucosal healing, and avoidance of disability.[3] And treatment for UC consists mainly of mesalazine, corticosteroids, immunosuppressive drugs and biological agents.[4]

https://doi.org/10.2147/CEG.S595836
Received: 13 January 2026
Accepted: 6 April 2026
Published: 30 April 2026

© 2026 Cui et al. This work is published and licensed by Dove Medical Press Limited. The full terms of this license are available at https://www.dovepress.com/terms.php and incorporate the Creative Commons Attribution – Non Commercial (unported, v4.0) License (http://creativecommons.org/licenses/by-nc/4.0/). By accessing the work you hereby accept the Terms. Non-commercial uses of the work are permitted without any further permission from Dove Medical Press Limited, provided the work is properly attributed. For permission for commercial use of this work, please see paragraphs 4.2 and 5 of our Terms (https://www.dovepress.com/terms.php).

Graphical Abstract

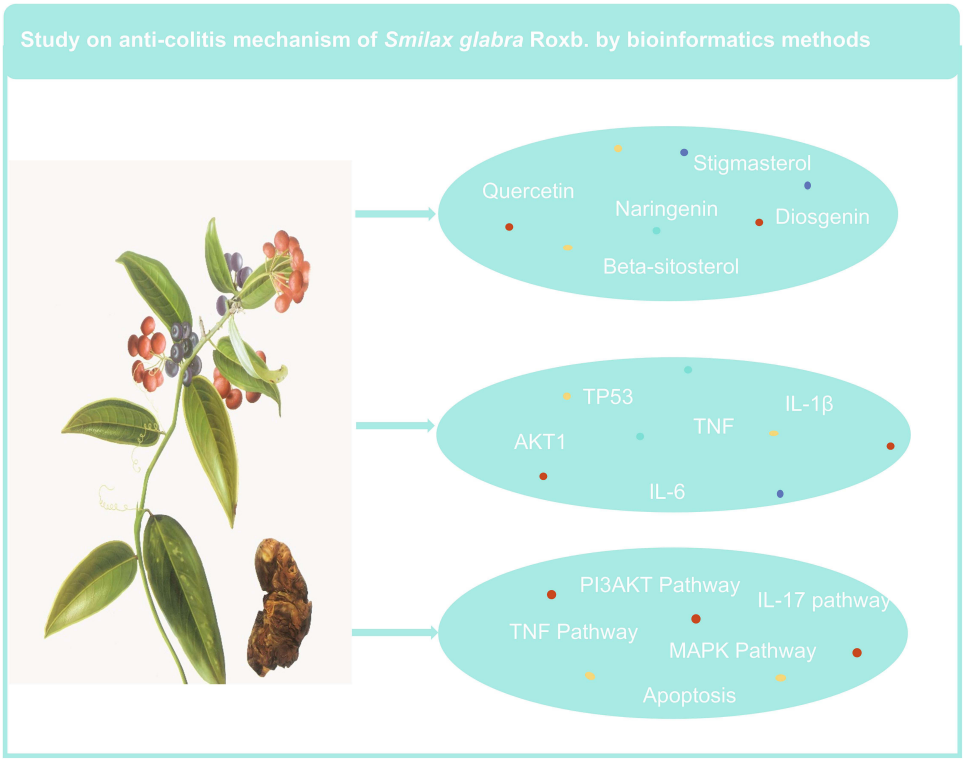

The Tp53 protein, acting as a transcription factor, is involved in DNA repair, cellular senescence, cell cycle regulation, autophagy and apoptosis.[5] TP53 gene is a key factor in the development of cancer and is regarded as the most important tumor suppressor gene. However, mutations in the TP53 gene are the most common mutations found in dysplastic lesions and cancers associated with IBD.[6] Compared with the normal control group or sporadic colorectal cancer, TP53 exhibits strong and uniform expression in the nuclei of inflammatory colorectal cancer cells, and its expression levels increase with the intensity of inflammation.[7] Akt1 is a subfamily of the AGC protein serine/threonine kinase family and plays a crucial role in cell growth, metabolic regulation, cancer, and other diseases.[8] Akt may be involved in UC by regulating inflammatory responses, cell proliferation, autophagy, and oxidative stress. AKT1 plays a role in autophagy and its regulatory mechanisms, contributes to the maintenance and repair of intestinal homeostasis, and supports intestinal barrier function during cellular stress by regulating tight junctions and preventing cell death.[9] Besides, Akt1 plays a crucial role in acute inflammation, primarily by regulating vascular permeability, thereby leading to oedema and leukocyte extravasation.[10] Thus, we hypothesize that TP53 and AKT1 play a particularly important role in the pathophysiology of UC.

Traditional Chinese Medicine (TCM) has unique medical theory and rich practical experience. There is a great variety of Chinese materia medica, including plants, animal parts and minerals. Among these materials, flowers, herbs and plants are the ones most frequently used that is why Chinese materia medica is called Chinese medicinal herbs. *Smilax glabra* Roxb. (SG), Chinese name Tufuling, is the dried rhizome of Liliaceae plant. The plant name has been verified with MPNS (http://mpns.kew.org). SG was first recorded in Ben Cao Jing Ji Zhu during the Southern and Northern Dynasties (420–589 AD) by Tao Hongjing.[11] Its' effects were anti-infective,[12,13] removing rheumatism, facilitating urination, stopping diarrhea, and treating muscles and bones. And it is also used to treat syphilitic poisoned sores, hypertonicity of the limbs, morbid leucorrhea, eczema pruritus, heat-induced strangury, carbuncle toxins, and many other conditions

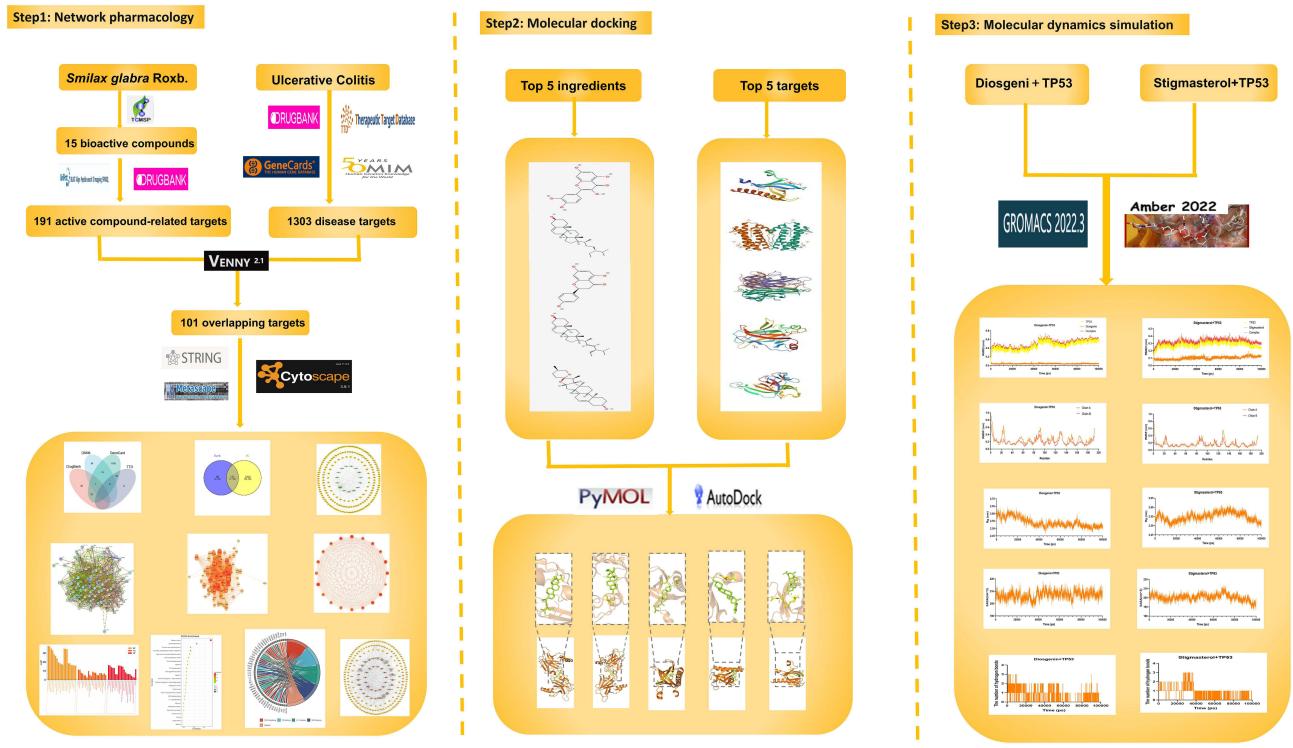

Figure 1 Framework diagram of this study.

(Editorial Committee of Zhong Hua Ben Cao, 1999).[14] Moreover, Professor Shen often uses SG to protect against UC by oral or enema administration in clinical practice. Surprisingly, SG can obviously relieve UC patients' abdominal pain and diarrhea.

Chinese herbs have the features of complex chemical composition, multi-target and multi-pathway. Network pharmacology pays attention to the integrity, systematization and interaction, so it is often used to investigate the mechanism of action of TCM.[15] Network pharmacology provides new ideas for the discovery and research of new drugs mainly by predicting drug components, therapeutic targets and potential mechanisms. Molecular docking is based on the results of network pharmacology to verify whether the ligand and receptor can bind and the binding energy value. Additionally, molecular dynamics simulation (MDs) can provide a detailed situation of the internal motion of biological macromolecules such as proteins and nucleic acids over time, that is, information such as structural fluctuations and conformational changes of proteins or macromolecules can be obtained from the microscopic level.[16]

Although SG is believed to be promising to treat UC, there is currently a lack of research into the mechanisms of SG for treating UC. Therefore, we designed this study to investigate the potential mechanisms underlying SG therapy for ulcerative colitis (Figure 1).

Material and Methods

Identification of Active Compounds and Gene Targets of SG

Using Chinese name "Tufuling", We employed the TCMSP (https://old.tcmsp-e.com/tcmsp.php) to search for the active components of SG, followed by screening the ideal components based on OB > 30% and DL > 0.18.[17] The corresponding targets of the active components were then obtained by MOLID. The human gene names were obtained from the Uniprot database (https://www.uniprot.org/)[18] and then targets of SG were matched with the human gene name via VLOOKUP function. The gene names of unmatched targets were searched in Uniprot (https://www.uniprot.org/) and Drugbank (https://go.drugbank.com/) databases.

https://doi.org/10.2147/CEG.S595836

Establishment of "Ingredient-Target" Network

After conducting the node and edge files, the data were entered into cytoscape3.9.1 to construct a "Ingredient-Target" network.[19] And made an adjustment of color, shape, size, and transparency based on degree value (the number of gene connections) for further visualization.

Acquisition of UC Targets

With "ulcerative colitis" as the key word, disease targets were predicted in OMIM (https://omim.org/),[20] TTD (http://db.idrblab.net/ttd/),[21] Drugbank (https://go.drugbank.com/) and Genecard (https://www.genecards.org/).[22] Subsequently, the targets of above databases were intersected through Venny software (https://bioinfogp.cnb.csic.es/). After removing duplicate items of disease targets, the intersection targets of the active compounds from SG and UC disease targets were obtained, which could act as potential targets against UC.

Construction of Protein-Protein Interaction Network

After uploading drug and disease overlapping targets to STRING 11.5 (https://cn.string-db.org/), "species" was limited to "Homo sapiens" and interaction score was set as greater than 0.4.[23] The result was further visualized using Cytoscope. Besides, pivotal targets of SG in the treatment of UC were screened according to degree value.

Enrichment Analysis of GO Function and KEGG Pathway

GO enrichment analysis was used to standardize the description of gene products from CC, MF and BP. KEGG is functional enrichment, and multiple genes may be significantly concentrated on which functions. Data were processed and imported into Metascape (https://metascape.org/) for GO and KEGG enrichment analysis. Subsequently, every top 20 terms in BP, CC, and MF and top 25 pathways in KEGG were uploaded to the Bioinformatics platform (http://www.bioinformatics.com.cn/) for visual analysis.[24]

Performance of Molecular Docking

Perform molecular docking based on network pharmacology data to evaluate the binding energies of the top 5 components with the target respectively. Obtain protein PDB files from the PDB database (https://www.rcsb.org/), remove water and solvent from the proteins using PyMol software, add hydrogen atoms using AutoDock4, set the proteins as receptors, and save them in PDBQT format. Acquire component MOL2 files from TCMSP, add hydrogen atoms to the compounds in AutoDock4, designate them as ligands, automatically configure the torsion tree, and save them in PDBQT format. Perform docking between the receptor PDBQT file and the ligand PDBQT file through AutoDock4, adjusting the Grid Box size to cover the active site. Set the molecular docking parameters, run genetic algorithm 50 times,[25] and select the result with the lowest binding energy for visualization using PyMol. It is commonly held that binding energies of less than −4.25 kcal/mol, −5.0 kcal/mol or −7.0 kcal/mol indicate certain, good or strong binding affinity between the ligand and the receptor, respectively.[26,27] The molecular docking experiments were repeated three times, with the lowest binding energy from each result selected for statistical analysis. The results are presented as the Mean ± SD.

Verification of Molecular Dynamics Simulation

This study employed the GROMACS 2022.3 software to perform molecular dynamics simulations.[28] For small-molecule pre-processing, AmberTools 22 is used to add the GAFF force field to the small molecules, alongside employing Gaussian 16W to perform hydrogenation and calculate RESP charges. The charge data is then incorporated into the molecular dynamics system's topology file. The simulations were conducted at a static temperature of 300 K and standard atmospheric pressure (1 bar). The force field adopted the Amber99sb-ILDN model, with water molecules (TIP3P water model) used as the solvent; an appropriate number of Na^+ ions were added to neutralize the total charge of the simulated system.

The molecular dynamics simulation system first employed the steepest descent method for energy minimization, subsequently performing 100,000 steps of both NVT (Constant Volume and Temperature) and NPT (Constant

Temperature and Pressure) ensemble equilibrations, with a coupling constant of 0.1 ps and a duration of 100 ps. Finally, a free molecular dynamics simulation was run, comprising 5,000,000 steps with a step size of 2 fs, resulting in a total duration of 100 ns. After completing the simulation, the software's built-in tools were used to analyse the trajectories, calculating the root-mean-square deviation (RMSD), root-mean-square fluctuation (RMSF) and radius of gyration (Rg) for each amino acid's motion trajectory, in conjunction with data such as the free energy.

Results

Active Compounds and Gene Targets of SG

A total of 74 compounds were shown in the Traditional Chinese Medicine Systems Pharmacology Database and Analysis Platform (TCMSP), among which 15 ingredients satisfied the oral bioavailability (OB) ≥ 30% and drug-likeness (DL) ≥ 0.18 (Table 1 and Supplementary Table 1). The respective protein targets were subsequently searched in the TCMSP database based on the MOLID of the 15 components, followed by transformation into gene symbol for normalization through UniProt database. The elimination of duplicated genes of 15 components resulted in 191 final gene targets (Supplementary Table 2).

"Ingredient-Target" Network

To clearly illustrate the relationship between 15 active ingredients and 191 potential targets in SG, a "Ingredient-Target" network was built, consisting of 206 nodes and 283 edges (Figure 2A). The node with more edges in the network has higher degree value, and the larger the size of the node, the greater the meaning. The top 5 compound nodes with the largest size of degree were quercetin (MOL000098), beta-sitosterol (MOL000358), naringenin (MOL004328), Stigmasterol (MOL000449), and diosgenin (MOL000546). The data was shown in Table 2.

Available Targets for UC

With "ulcerative colitis" as key word, 1552 disease targets acquired from GeneCards, OMIM, Drugbank and TTD databases after screening (Figure 2B). Ultimately, 1303 disease targets without duplication were identified. Upload 191 active compound-related targets and 1303 UC-related targets into Venny 2.1.0 website for the purpose of retaining 101 overlapping targets as candidate targets (Figure 2C).

Table 1 15 Active Ingredients of *Smilax glabra* Roxb

Mol ID	Molecule Name	Molecule Weight	Pubchem Cid	OB (%)	DL
MOL000098	Quercetin	302.25	5,280,343	46.43	0.28
MOL000358	Beta-sitosterol	414.79	222,284	36.91	0.75
MOL004328	Naringenin	272.27	439,246	59.29	0.21
MOL000449	Stigmasterol	412.77	5,280,794	43.83	0.76
MOL000546	Diosgenin	414.69	99,474	80.88	0.81
MOL004576	Taxifolin	304.37	439,533	57.84	0.27
MOL013117	4,7-Dihydroxy-5-methoxyl-6-methyl-8-formyl-flavan	314.36	129,394	37.03	0.28
MOL004580	Cis-Dihydroquercetin	304.27	443,758	66.44	0.27
MOL013129	(2R,3R)-2-(3,5-dihydroxyphenyl)-3,5,7-trihydroxychroman-4-one	304.27	5,320,468	63.17	0.27
MOL001736	(-)-taxifolin	304.27	712,613	60.51	0.27
MOL000359	Sitosterol	414.79	12,303,645	36.91	0.75
MOL004575	Astilbin	450.43	119,258	36.46	0.74
MOL013118	Neoastilbin	450.43	442,437	40.54	0.74
MOL013119	Enhydrin	464.51	5,281,441	40.56	0.74
MOL004567	Isoengelitin	434.43	12,309,470	34.65	0.7

https://doi.org/10.2147/CEG.S595836

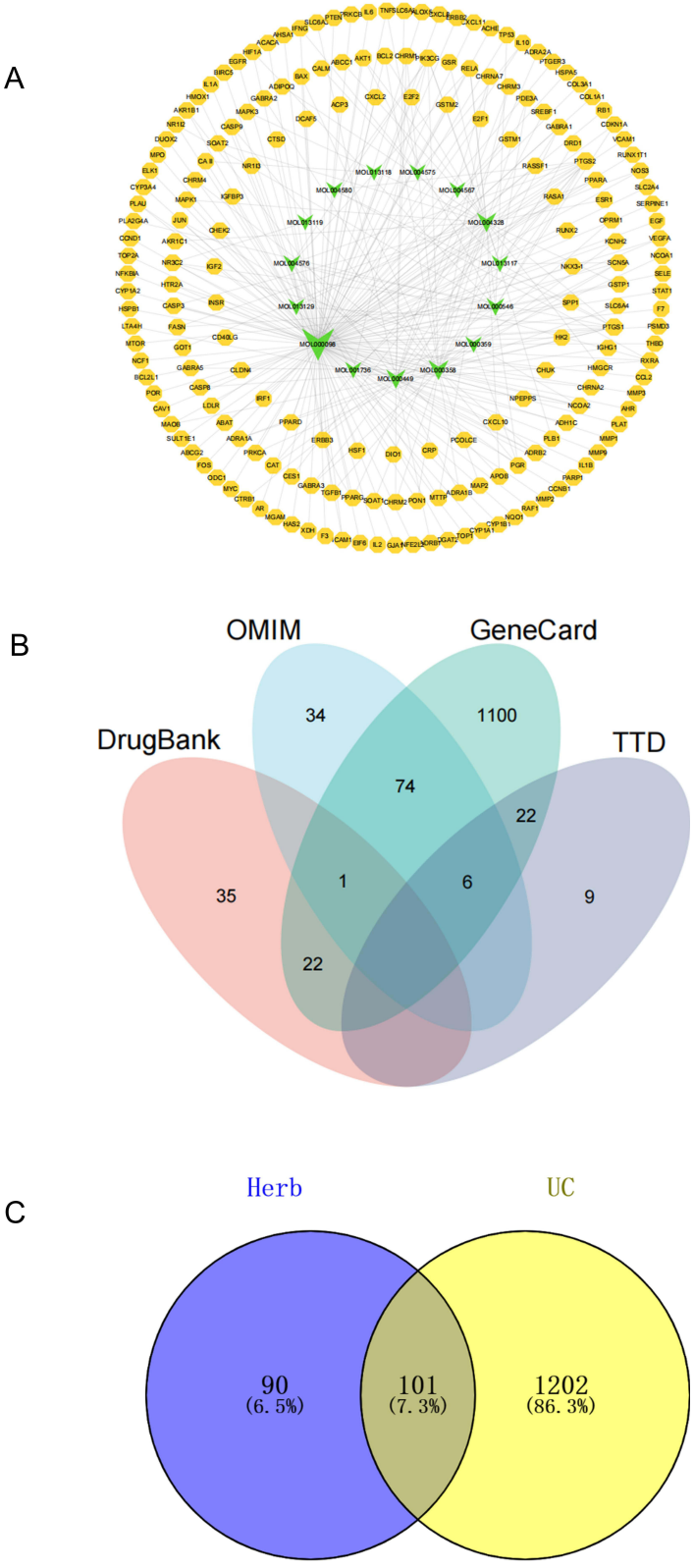

Figure 2 Potential targets of SG against UC. (**A**) Ingredient-Target network of SG. Green **V** indicates ingredients. Orange octagons show target. The color and size of the nodes reflect the degree value. Grey lines indicate the interrelationships between compounds and targets. (**B**) Distribution of UC targets in OMIM, TTD, Drugbank, and Genecard. (**C**) Distribution of SG targets and UC targets.

Table 2 Top 5 Ingredients of *Smilax glabra* Roxb

Molecule Name	Structure	Degree	Betweenness Centrality	Closeness Centrality
Quercetin	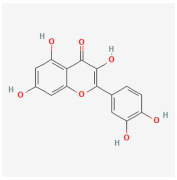	141	0.83	0.63
Beta-sitosterol	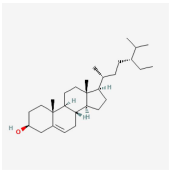	35	0.14	0.38
Naringenin	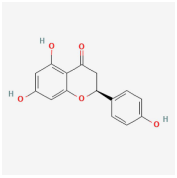	30	0.17	0.37
Stigmasterol	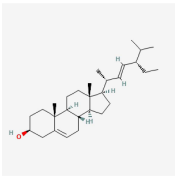	29	0.13	0.37
Diosgenin	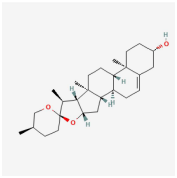	14	0.04	0.36

Protein-Protein Interaction

The 101 candidate targets were imported into STRING 11.5 to construct a PPI network, comprising 101 nodes and 2108 edges (Figure 3A). The data were imported into Cytoscape 3.9.1 for a visual PPI network, which also included 101 nodes and 2108 edges (Figure 3B). The top 20 targets, in the light of degree value, were selected to build core targets network map (Figure 3C). As shown, correlation is proportional to node size and color depth. The top 5 targets are AKT1, IL-6, TNF, TP53, IL-1β, which may be considered as key targets in the anti-UC pharmacological mechanism of SG (Table 3).

https://doi.org/10.2147/CEG.S595836

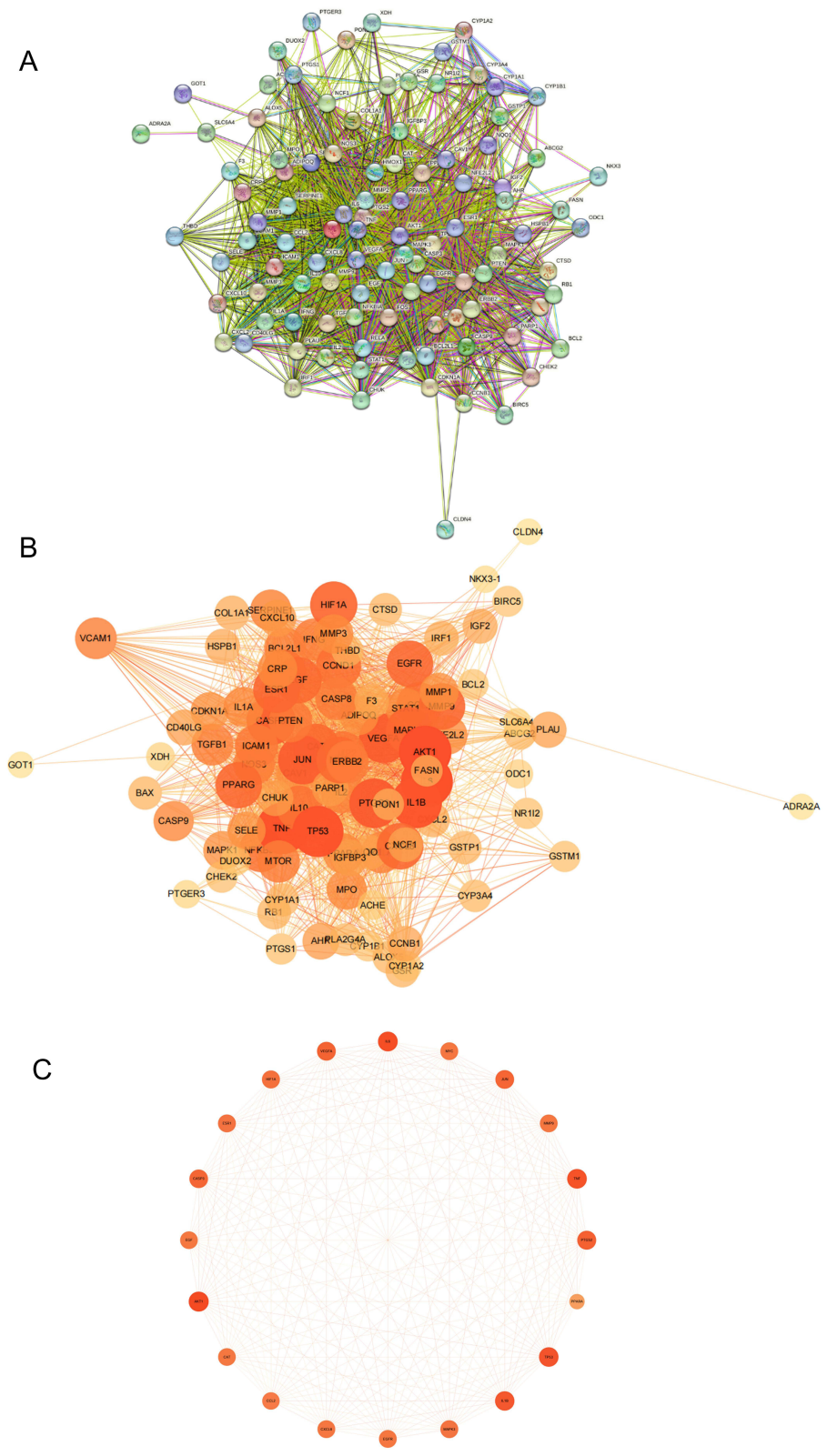

Figure 3 Protein-protein interaction. (**A**) The interactive PPI network obtained from STRING database with the minimum required interaction score set to 0.97. (**B**) PPI network imported from STRING database to Cytoscape 3.9.1. (**C**) PPI network of more significant proteins extracted from (b) by degree value.

Table 3 Top 5 Targets Information of PPI Network

Name	Structure	Degree	Betweenness Centrality	Closeness Centrality
AKT1		87	0.037	0.88
IL-6		85	0.04	0.87
TNF-α	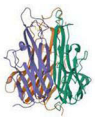	84	0.03	0.85
TP53		83	0.03	0.85
IL-1β		82	0.03	0.85

GO and KEGG Pathway Enrichment Analysis

The 101 SG–UC targets were imported into the Metascape and GO functional enrichment analysis was carried out on the targets of active compounds in the treatment of UC from the perspective of cellular component (CC), molecular function (MF) and biological process (BP). We obtained 1727 statistically significant GO items in total, including 1546 for BP, 50 for CC, and 131 for MF. The top 20 BP, CC and MF were visualized in a bar graph (Figure 4A). The significantly enriched BP terms associated with targets of SG were "response to inorganic substance", "response to oxidative stress", "response to reactive oxygen species". CC was concerned with "membrane raft", "membrane microdomain" and "caveola" and MF was related with "cytokine receptor binding", "cytokine activity" and "signaling receptor activator activity". Besides, 178 pathways were obtained by KEGG enrichment analysis, of which the top 25 pathways were presented in the form of bubble plots according to with the highest gene counts (Figure 4B). Among them, PI3K−Akt signaling pathway (associated with 24 genes), TNF signaling pathway (associated with 23 genes), IL-17 signaling pathway (associated with 21 genes), MAPK signaling pathway (associated with 21 genes) and apoptosis (associated with 19 genes) are closely related to UC (Figure 4C). Finally, we constructed a component-target-pathway network with 231 nodes and 871 edges to illustrate their relationships (Figure 4D).

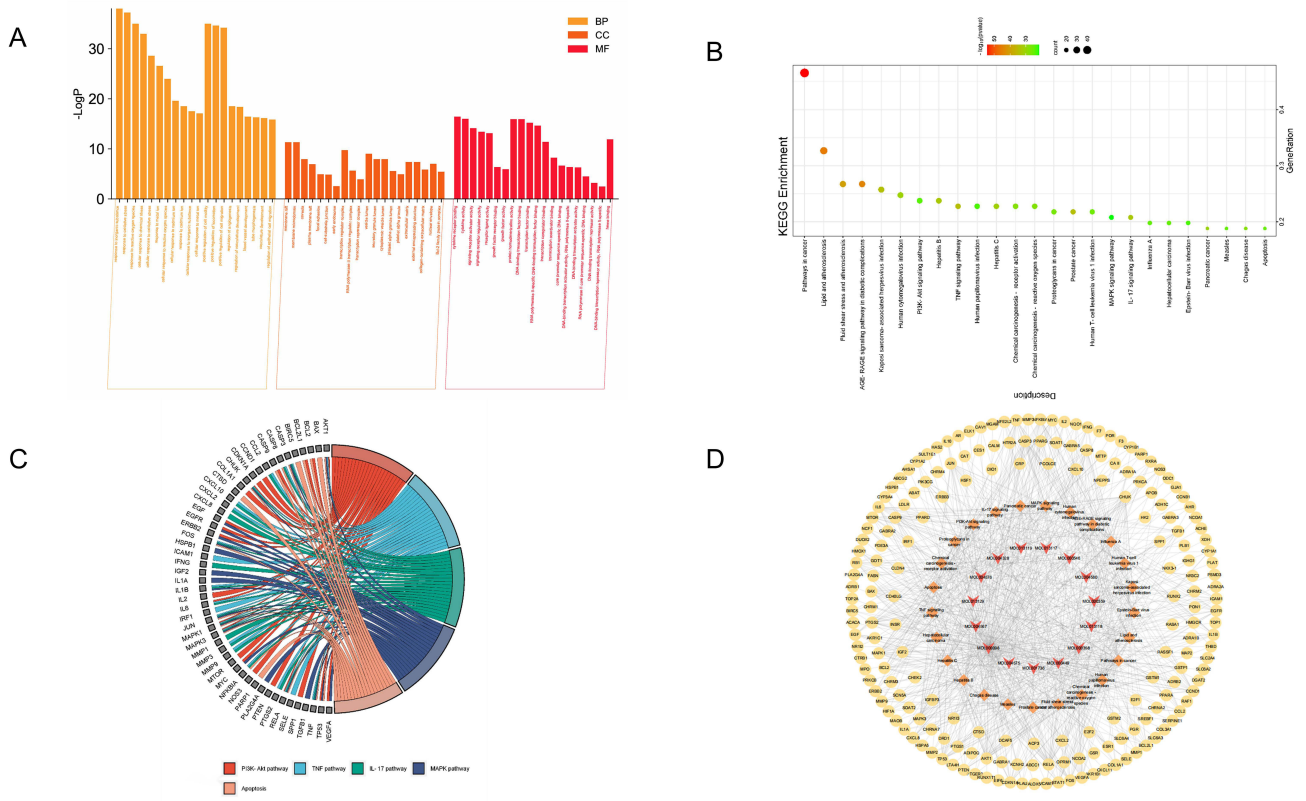

Figure 4 GO and KEGG Pathway Enrichment Analysis (**A**) GO enrichment analysis for 101 key targets. (**B**) KEGG enrichment analysis for 101 key targets. (**C**) Gene ontology of the 5 pathways in SG against UC. (**D**) Component-Target-Pathway network. Red **V** represents component. Yellow octagon shows target. Orange diamond represents pathway. The color and size of the nodes reflect the degree value. Grey lines indicate the interrelationships between compounds and targets.

Molecular Docking

Combined with the network pharmacology results, the top 5 components, quercetin (MOL000098), beta-sitosterol (MOL000358), naringenin (MOL004328), Stigmasterol (MOL000449), diosgenin (MOL000546), and top 5 protein targets, AKT1 (PDB ID: IUNQ), IL-6 (PDB ID: IALU), TNF (PDB ID: 1A8M), TP53 (PDB ID: 7DHZ), IL-1β (PDB ID: 3LTQ), were docked separately. Each set of molecular docking run was performed 50 times, repeated three times, making a total of 150 runs; the sample size is sufficient, and the results are statistically significant. Binding energy results are presented as Mean ± SD in Table 4, suggesting a lower score indicated a stabler binding state. The visualization of the top 5 protein-component complexes with the smallest binding energies is displayed in Figure 5A–E. The other 20 molecular docking data are displayed in Supplementary Figure 1. Stigmasterol can interact with ASN-247 through one hydrogen bond in TP53. The structure of diosgenin could form one hydrogen bond with SER-240 with TP53. The stigmasterol–AKT1 complex was stabilized by one hydrogen bond with GLU-91 and two hydrogen bonds with GLU-95.

Table 4 The Docking Scores (kcal/Mol) of the Active Compounds and Key Targets

ID	MOL000098	MOL000358	MOL004328	MOL000449	MOL000546
Target	Quercetin	Beta-sitosterol	Naringenin	Stigmasterol	Diosgenin
AKT1	−6.25 ± 0.32	−7.22 ± 0.63	−6.17 ± 0.04	−7.38 ± 0.72	−7.95 ± 0.06
IL6	−6.24 ± 0.44	−7.21 ± 0.01	−6.18 ± 0.03	−7.45 ± 0.26	−7.89 ± 0.15
TNF	−7.19 ± 2.4	−6.38 ± 0.71	−7.22 ± 1.78	−6.97 ± 0.74	−7.40 ± 0.04
TP53	−7.73 ± 1.29	−7.18 ± 1.29	−7.48 ± 1.10	−9.10 ± 0.07	−8.80 ± 0.73
IL1β	−6.44 ± 1.49	−6.98 ± 0.69	−6.53 ± 1.19	−7.13 ± 0.59	−7.49 ± 0.87

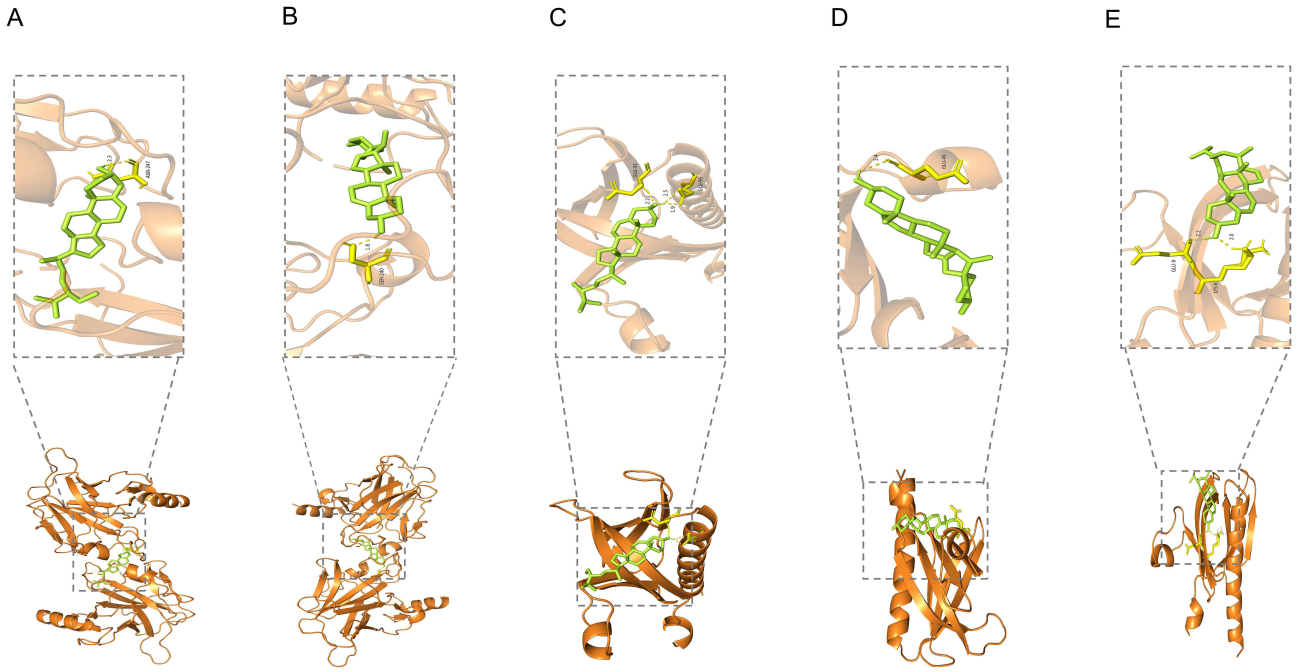

Figure 5 Molecular docking (**A**) Stigmasterol with TP53; (**B**) Diosgenin with TP53; (**C**) Stigmasterol with Akt1. (**D**) Diosgenin with Akt1 (**E**) Betasitosterol with Akt1. The hydrogen bonds were indicated by dashed lines and the length was added around the lines.

Diosgenin forms one hydrogen bond with GLU-49 in AKT1. Beta-sitosterol interacts with GLU-9 and LYS-8 through one hydrogen bond in AKT1.

Molecular Dynamics Simulation

We selected the top 2 compound–target dockings (stigmasterol–TP53 and diosgenin–TP53) to conduct the molecular dynamics simulations. After 100 ns of MDs, the dynamic evolutions of the stigmasterol–TP53 and diosgenin–TP53 complexes could be analyzed. The RMSD, an indicator of protein structural changes, was calculated for stigmasterol–TP53 and diosgenin–TP53. Although RMSD has certain fluctuations in the early stage, stigmasterol-TP53 stabilized after 20 ns while diosgenin-TP53 stabilized after 50 ns (Figure 6A and B). And RMSD of stigmasterol-TP53 was smaller than that of diosgenin-TP53, indicating that stigmasterol-TP53 was more stable This indicates that after the small molecule ligand is combined with the protein, the conformation of the protein will not change significantly, and the combination of the two is relatively stable.

In addition, RMSF is often used to assess protein dynamics. The results show that the RMSF of the protein is small in the bound part, but becomes large in the unbound part, manifesting that the binding of small molecules has some effect on the stability of the protein. The RMSF values of residue numbers 20–90 in the TP53 upon binding of diosgenin showed larger flexibility than the same regions in TP53 bound with stigmasterol (Figure 6C and D).

The Rg can represent the tightness of the protein structure. Diosgenin-TP53 and stigmasterol-TP53 have stable gyration radii (Figure 6E and F). This result is consistent with the RMSD result, meaning that the protein conformation is stable and is compactly folded. Furthermore, the binding of small molecules does not affect protein stability.

The solvent-accessible surface area (SASA) is often used to assess protein surface area. It was observed that the SASA fluctuation patterns of the diosgenin-TP53 and stigmasterol-TP53 systems were consistent throughout the simulation time (Figure 6G and H). HBond is an index for evaluating hydrogen bonds between proteins and small molecules. Hydrogen bonding and hydrophobic interaction play an important role in the preservation of protein conformation. The interaction binding sites of the diosgenin–TP53 and stigmasterol–TP53 formed hydrophilic environments with strong hydrophilicity, while the hydrogen bonds formed could help to maintain their stabilities (Figure 6I and J).

https://doi.org/10.2147/CEG.S595836

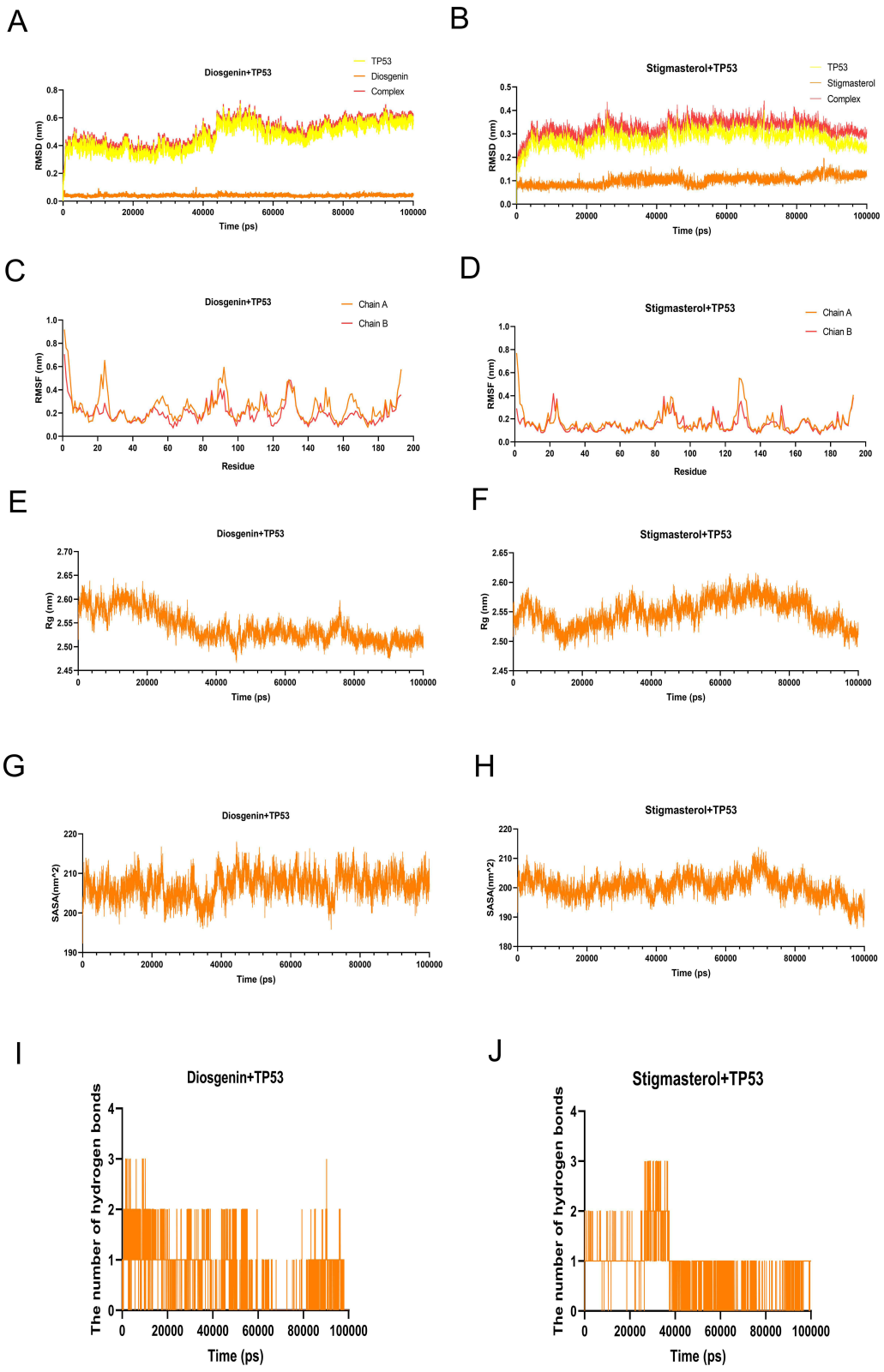

Figure 6 Molecular dynamics simulation. (**A** and **B**) RMSD curves; (**C** and **D**) RMSF curves; (**E** and **F**) Radius of rotation curves; (**G** and **H**) SASA curves; (**I** and **J**) Number of hydrogen bonds.

Table 5 Binding Energies of the Two Systems. Energy Values are Provided as kcal/Mol

Complex	ΔVDWAALS	ΔEEL	ΔGGAS	ΔGSOLV	ΔTOTAL
Stigmasterol–TP53	−55.22 ± 1.45	−12.89 ± 1.89	−68.11 ± 2.38	37.29 ± 0.08	−30.82 ± 2.38
Diosgenin–TP53	−64.23 ± 1.05	−7.04 ± 0.74	−71.27 ± 1.29	−52.99 ± 0.59	−18.28 ± 1.42

Abbreviations: ΔVDWAALS: vander Waals energy; ΔEEL: electrostatic energy; ΔGGAS: gas-phase free energy; ΔGSOLV: solvation free energy; ΔTOTAL: total binding free energy.

Moreover, more hydrogen bonds formed between the diosgenin–TP53 than between the Stigmasterol–TP53 during the 100 ns simulations. To judge whether the binding between proteins and small molecules is reasonable, we also need to evaluate some other indicators. One of the most commonly used indicators is Molecular mechanics Poisson–Boltzmann surface area (MMPBSA) analysis. By calculating the energy between the protein and the small molecule, we can obtain the total free energy of two complexes, and thus judge whether the binding between the protein and the small molecule is stable An energy convergence analysis was performed on 100 snapshots of the 100 ns simulations of each complex. Binding free energy is listed as Mean ± SD in Table 5. Taking the above results together, we can conclude that the interaction between proteins and small molecules is stable, and the binding of small molecules makes the protein molecules more compact, the surface area is reduced, and many hydrogen bonds are formed between proteins and small molecules.

Discussion

According to TCM theory, dampness-heat is an important factor in the occurrence and development of UC. Therefore, herbs for clearing heat and removing dampness are used to treat UC, and SG is one of the representative herbs. In recent years, there has been an increasing number of studies on the active ingredients of SG, and studies have shown that flavonoids,[29,30] phenolic and phenolic aids,[11] stilbene and organic acids[31] and phenylpropanoid are the most extensively studied bioactive components and are considered essential active components. Pharmacological studies have proven that SG have a variety of effects, including anti-cancer,[32,33] anti-inflammatory,[34,35] antioxidant.[36] Moreover, the role of SG in the treatment of various diseases has also been intensively studied. SG may protect against pathological cardiac hypertrophy via negative regulation of the Raf/MEK/ERK pathway.[37] SG inhibited collagen induced adhesion and migration of PC3 and LNCaP prostate cancer cells through the inhibition of Beta 1 integrin expression.[38] Ethyl acetate in SG played an anti-tumor role by inhibiting the activation of the HIF-1 signaling pathway and response by resetting tumor-associated macrophages toward the M1 phenotype.[39]

Given the paucity of study on the treatment of UC with SG, the possible mechanism of SG against UC was revealed using comprehensive network pharmacology and further verified by molecular docking and MDs. The 15 active compounds, 191 targets associated with compounds were identified. The top 5 compounds were quercetin (MOL000098), beta-sitosterol (MOL000358), naringenin (MOL004328), Stigmasterol (MOL000449), and diosgenin (MOL000546). A total of 101 overlapping targets were obtained after matching 191 component-related targets with 1303 disease-related targets. These results confirmed that Chinese herbal medicine exerts its anti-UC effect through multiple components and targets.

The PPI analysis of the 101 targets shows that the top 10 central targets, including AKT1, IL-6, TNF, TP53, IL-1β, PTGS2, VEGFA, JUN, CASP3 and HIF1A, may be the key targets of the treatment of UC. Therefore, the top 5 components and top 5 targets were selected for molecular docking separately. The binding energy of molecular docking indicated that the active ingredient and protein target were bound stably. To further explore the anti-UC effect of SG in depth, GO and KEGG analyses were performed. GO results showed that the target genes of BP were mainly enriched in reactive oxygen species and oxidative stress. Oxygen metabolism necessary for mammalian cell survival generates reactive oxygen species.[40] Oxidative Stress refers to a state of imbalance between oxidation and antioxidation in the body, which tends to oxidation, leading to inflammatory infiltration of neutrophils, increased secretion of protease, and production of a large number of oxidative intermediates.[41] Existing studies have shown that oxidative stress can participate in multiple levels of function and promote IBD.[42,43] In other aspects, MF mainly involves cytokine receptor

binding and cytokine activity. The PI3K−Akt signaling pathway has a significant effect on UC. Studies have shown that the glucose-dependent anti-inflammatory properties of mesenchymal stem/stromal cells conferred by inflammatory factors are mediated by PI3K-AKT signaling pathway.[44] As TNF and IL17 are classical inflammatory pathways in UC, we will not repeat them. MAPK pathway also is closely associated with inflammatory response and generally activated by Toll-like receptors.[45] SG could alleviate psoriasis-like dermatitis by reducing the expression of cytokines and chemokines mediated by the MAPK pathway, and improved amino acid and carnitine metabolism in vivo.[46] Apoptosis is essential for the development and maintenance of cellular homeostasis. Intestinal epithelial cells derived from crypt floor stem cells have a lifespan of less than a week, and they often die on the luminal surface due to apoptosis.[47] Therefore, the relationship between UC and apoptosis has been studied, such as the demonstration that 3-mercaptopyruvate sulfurtransferase may protect the intestines from inflammation most likely by regulating the AKT/apoptosis axis in intestinal epithelial cells.[48] These findings could support our KEGG pathway enrichment analysis.

The results of 25 molecular docking showed that the top 5 components and targets could dock. We selected the 2 complexes, Stigmasterol–TP53 and diosgenin–TP53, with the lowest binding energy for MDs. MMPBSA is generally considered to offer greater computational accuracy, making the prediction of binding free energy using the MMPBSA method theoretically more rigorous. The results of MDs show the binding free energy value of stigmasterol–TP53 (−30.82 ± 2.38 kcal/mol) and diosgenin–TP53 (−18.28 ± 1.42 kcal/mol) are significantly more meaningful than the affinities acquired from AutoDock4. Based on the results of the computational experiments, we hypothesize that TP53 may be the most promising target for SG therapy in UC. There have been some studies to date exploring the relationship between UC and TP53. In non-cancerous IBD samples, TP53 was observed to be expressed in a focal or diffuse pattern in 81.8% of samples, with a higher proportion of TP53-positive cells in samples exhibiting the most severe inflammation.[7] A study has shown that Tp53 is present in the nuclei of almost all cells in regenerating crypts of UC mice, whereas it is almost entirely absent in epithelial cells during homeostasis, suggesting that Tp53 signaling is activated after colitis-associated injury.[49] During the ongoing regeneration process in Tp53 conditional knockout mice, abnormalities in epithelial structure and barrier function are observed, manifested by a failure to restore crypt architecture, reduced mucus secretion, and impaired mucosal barrier function, leading to a vicious cycle of exacerbated intestinal inflammation.[49] Despite being dispensable for the maintenance of epithelial homeostasis, Tp53 plays a crucial role in the transition of epithelial cells from the regenerative phase back to homeostasis following colitis-related injury. If cells lacking Tp53 enter a proliferative state, they are unable to exit that state.[49] Their heightened proliferative potential may prevent the involved epithelium from restoring homeostasis, causing it to remain highly proliferative and exhibit chronic inflammation and immune infiltration.[49] The loss of normal signal transduction may lead to progressive functional dysfunction, chronic colitis, and ultimately carcinogenesis.[50] TP53 is the most frequently mutated gene in human malignancies, 50% of which carry alterations to it.[51] Mutations in Tp53 that go along with loss of Tp53 signaling are observed earlier and more frequently in UC-associated colorectal cancer.[52,53] The high proportion of UC-associated tumors with loss-of-function or dominant-negative mutations of Tp53 combined with a loss of heterozygosity.[54,55] These loss-of-function mutations in Tp53 have been identified as potential drivers of carcinogenesis in UC patients.[54] Therefore, patients with chronic IBD may be at increased risk of developing colorectal cancer. Our results suggest that SG may be a potential treatment for TP53-mutated UC and colorectal cancer associated with UC. It should be noted that the findings mentioned above are merely preliminary results obtained through bioinformatics analysis and still require further validation through animal and cell experiments.

Conclusion

This study is the first to investigate the active constituents of SG and possible mechanisms against UC using network pharmacology and molecular analysis. Novelty of this study lies in linking SG compounds to UC-specific targets and confirming stable docking/MDs interactions with TP53. However, a limitation of this study lies in the fact that these results were obtained entirely through computational methods and lack experimental validation. Further in vivo and in vitro experiments are therefore required to confirm these findings.

Abbreviations

SG, *Smilax glabra* Roxb.; UC, ulcerative colitis; MDs, molecular dynamics simulations; IBD, inflammatory bowel disease; TCM, Traditional Chinese Medicine; TCMSP, Traditional Chinese Medicine Systems Pharmacology Database and Analysis Platform; OB, oral bioavailability; DL, drug-likeness; CC, cellular component; MF, molecular function; BP, biological process; NVT, Constant Volume and Temperature; NPT, Constant Temperature and Pressure; RMSD, root-mean-square variance; RMSF, root-mean-square fluctuation; Rg, radius of gyros; MMPBSA, Molecular mechanics Poisson–Boltzmann surface area; SASA, solvent-accessible surface area; OS, Oxidative Stress.

Ethics Statement

All databases in this study are public databases, the contents of which are publicly available and allow unrestricted reuse through open licenses. According to official document issued by National Science and Technology Ethics Committee of China, the use of legally obtained public data is not subject to ethical scrutiny (https://www.gov.cn/zhengce/zhengceku/2023-02/28/content_5743658.htm).

Acknowledgments

This research received no external funding.

Author Contributions

All authors made a significant contribution to the work reported, whether that is in the conception, study design, execution, acquisition of data, analysis and interpretation, or in all these areas; took part in drafting, revising or critically reviewing the article; gave final approval of the version to be published; have agreed on the journal to which the article has been submitted; and agree to be accountable for all aspects of the work.

Disclosure

The authors declare no conflict of interest.

References

1. Ordás I, Eckmann L, Talamini M, Baumgart DC, Sandborn WJ. Ulcerative colitis. *Lancet*. 2012;380(9853):1606–1619. doi:10.1016/S0140-6736(12)60150-0
2. Danese S, Fiocchi C. Ulcerative colitis. *N Engl J Med*. 2011;365(18):1713–1725. doi:10.1056/NEJMra1102942
3. Vind I, Riis L, Jess T, et al. Increasing incidences of inflammatory bowel disease and decreasing surgery rates in Copenhagen City and County, 2003–2005: a population-based study from the Danish Crohn colitis database. *Am J Gastroenterol*. 2006;101(6):1274–1282. doi:10.1111/j.1572-0241.2006.00552.x
4. Ungaro R, Mehandru S, Allen PB, Peyrin-Biroulet L, Colombel JF. Ulcerative colitis. *Lancet*. 2017;389(10080):1756–1770. doi:10.1016/S0140-6736(16)32126-2
5. Voskarides K, Giannopoulou N. The Role of TP53 in Adaptation and Evolution. *Cells*. 2023;12(3):512. doi:10.3390/cells12030512
6. Wanders LK, Cordes M, Voorham Q, et al. IBD-Associated Dysplastic Lesions Show More Chromosomal Instability Than Sporadic Adenomas. *Inflamm Bowel Dis*. 2020;26(2):167–180. doi:10.1093/ibd/izz171
7. Laurent C, Svrcek M, Flejou JF, et al. Immunohistochemical expression of CDX2, β-catenin, and TP53 in inflammatory bowel disease-associated colorectal cancer. *Inflamm Bowel Dis*. 2011;17(1):232–240. doi:10.1002/ibd.21451
8. Cole PA, Chu N, Salguero AL, Bae H. AKTivation mechanisms. *Curr Opin Struct Biol*. 2019;59:47–53. doi:10.1016/j.sbi.2019.02.004
9. Foerster EG, Mukherjee T, Cabral-Fernandes L, Rocha JDB, Girardin SE, Philpott DJ. How autophagy controls the intestinal epithelial barrier. *Autophagy*. 2022;18(1):86–103. doi:10.1080/15548627.2021.1909406
10. Di Lorenzo A, Fernández-Hernando C, Cirino G, Sessa WC. Akt1 is critical for acute inflammation and histamine-mediated vascular leakage. *Proc Natl Acad Sci U S A*. 2009;106(34):14552–14557. doi:10.1073/pnas.0904073106
11. Wu H, Wang Y, Zhang B, et al. Smilax glabra Roxb.: a Review of Its Traditional Usages, Phytochemical Constituents, Pharmacological Properties, and Clinical Applications. *Drug Des Devel Ther*. 2022;16:3621–3643. doi:10.2147/DDDT.S374439
12. Ooi LS, Sun SS, Wang H, Ooi VE. New mannose-binding lectin isolated from the rhizome of Sarsaparilla Smilax glabra Roxb. (Liliaceae). *J Agric Food Chem*. 2004;52(20):6091–6095. doi:10.1021/jf030837o
13. Tewtrakul S, Itharat A, Rattanasuwan P. Anti-HIV-1 protease- and HIV-1 integrase activities of Thai medicinal plants known as Hua-Khao-Yen. *J Ethnopharmacol*. 2006;105(1–2):312–315. doi:10.1016/j.jep.2005.11.021
14. Hua S, Zhang Y, Liu J, et al. Ethnomedicine, Phytochemistry and Pharmacology of Smilax glabra: an Important Traditional Chinese Medicine. *Am J Chin Med*. 2018;46(2):261–297. doi:10.1142/S0192415X18500143
15. Nogales C, Mamdouh ZM, List M, Kiel C, Casas AI, Schmidt H. Network pharmacology: curing causal mechanisms instead of treating symptoms. *Trends Pharmacol Sci*. 2022;43(2):136–150. doi:10.1016/j.tips.2021.11.004

16. Hollingsworth SA, Dror RO. Molecular Dynamics Simulation for All. *Neuron*. 2018;99(6):1129–1143. doi:10.1016/j.neuron.2018.08.011
17. Jiao Y, Shi C, Sun Y. Unraveling the Role of Scutellaria baicalensis for the Treatment of Breast Cancer Using Network Pharmacology, Molecular Docking, and Molecular Dynamics Simulation. *Int J Mol Sci*. 2023;24(4):3594. doi:10.3390/ijms24043594
18. Ding P, Liu J, Li Q, et al. Investigation of the Active Ingredients and Mechanism of Hudi Enteric-Coated Capsules in DSS-Induced Ulcerative Colitis Mice Based on Network Pharmacology and Experimental Verification. *Drug Des Devel Ther*. 2021;15:4259–4273. doi:10.2147/DDDT.S326029
19. Otasek D, Morris JH, Bouças J, Pico AR, Demchak B. Cytoscape Automation: empowering workflow-based network analysis. *Genome Biol*. 2019;20(1):185. doi:10.1186/s13059-019-1758-4
20. Amberger JS, Bocchini CA, Schiettecatte F, Scott AF, Hamosh A. OMIM.org: online Mendelian Inheritance in Man (OMIM®), an online catalog of human genes and genetic disorders. *Nucleic Acids Res*. 2015;43(Database issue):D789–D798. doi:10.1093/nar/gku1205
21. Wang Y, Zhang S, Li F, et al. Therapeutic target database 2020: enriched resource for facilitating research and early development of targeted therapeutics. *Nucleic Acids Res*. 2020;48(D1):D1031–D1041. doi:10.1093/nar/gkz981
22. Rebhan M, Chalifa-Caspi V, Prilusky J, Lancet D. GeneCards: integrating information about genes, proteins and diseases. *Trends Genet*. 1997;13(4):163. doi:10.1016/S0168-9525(97)01103-7
23. Szklarczyk D, Gable AL, Lyon D, et al. STRING v11: protein-protein association networks with increased coverage, supporting functional discovery in genome-wide experimental datasets. *Nucleic Acids Res*. 2019;47(D1):D607–D613. doi:10.1093/nar/gky1131
24. Li X, Wei S, Niu S, et al. Network pharmacology prediction and molecular docking-based strategy to explore the potential mechanism of Huanglian Jiedu Decoction against sepsis. *Comput Biol Med*. 2022;144:105389. doi:10.1016/j.compbiomed.2022.105389
25. Nguyen NT, Nguyen TH, Pham TNH, et al. Autodock Vina Adopts More Accurate Binding Poses but Autodock4 Forms Better Binding Affinity. *J Chem Inf Model*. 2020;60(1):204–211. doi:10.1021/acs.jcim.9b00778
26. Liu J, Liu J, Tong X, et al. Network Pharmacology Prediction and Molecular Docking-Based Strategy to Discover the Potential Pharmacological Mechanism of Huai Hua San Against Ulcerative Colitis. *Drug Des Devel Ther*. 2021;15:3255–3276. doi:10.2147/DDDT.S319786
27. Zhang S, Yang Y, Zhang R, et al. The Potential Mechanism of Alpiniae oxyphyllae Fructus Against Hyperuricemia: an Integration of Network Pharmacology, Molecular Docking, Molecular Dynamics Simulation, and In Vitro Experiments. *Nutrients*. 2024;17(1):71. doi:10.3390/nu17010071
28. Van Der Spoel D, Lindahl E, Hess B, Groenhof G, Mark AE, Berendsen HJ. GROMACS: fast, flexible, and free. *J Comput Chem*. 2005;26(16):1701–1718. doi:10.1002/jcc.20291
29. Xu S, Shang MY, Liu GX, et al. Chemical constituents from the rhizomes of *Smilax glabra* and their antimicrobial activity. *Molecules*. 2013;18(5):5265–5287. doi:10.3390/molecules18055265
30. Shu J, Li L, Zhou M, et al. Three new flavonoid glycosides from *Smilax glabra* and their anti-inflammatory activity. *Nat Prod Res*. 2018;32(15):1760–1768. doi:10.1080/14786419.2017.1402314
31. Chen T, Li J, Cao J, Xu Q, Komatsu K, Namba T. A new flavanone isolated from rhizoma smilacis glabrae and the structural requirements of its derivatives for preventing immunological hepatocyte damage. *Planta Med*. 1999;65(1):56–59. doi:10.1055/s-1999-13963
32. She T, Zhao C, Feng J, et al. Sarsaparilla (*Smilax Glabra* Rhizome) extract inhibits migration and invasion of cancer cells by suppressing TGF-β1 pathway. *PLoS One*. 2015;10(3):e0118287. doi:10.1371/journal.pone.0118287
33. Gao Y, Su Y, Qu L, et al. Mitochondrial apoptosis contributes to the anti-cancer effect of *Smilax glabra* Roxb. *Toxicol Lett*. 2011;207(2):112–120. doi:10.1016/j.toxlet.2011.08.024
34. Jiang J, Wu F, Lu J, Lu Z, Xu Q. Anti-inflammatory activity of the aqueous extract from Rhizoma smilacis glabrae. *Pharmacol Res*. 1997;36(4):309–314. doi:10.1006/phrs.1997.0234
35. Jiang J, Xu Q. Immunomodulatory activity of the aqueous extract from rhizome of *Smilax glabra* in the later phase of adjuvant-induced arthritis in rats. *J Ethnopharmacol*. 2003;85(1):53–59. doi:10.1016/S0378-8741(02)00340-9
36. Zhao X, Chen R, Shi Y, Zhang X, Tian C, Xia D. Antioxidant and Anti-Inflammatory Activities of Six Flavonoids from *Smilax glabra* Roxb. *Molecules*. 2020;25(22):5295. doi:10.3390/molecules25225295
37. Fu D, Zhou J, Xu S, et al. *Smilax glabra* Roxb. flavonoids protect against pathological cardiac hypertrophy by inhibiting the Raf/MEK/ERK pathway: in vivo and in vitro studies. *J Ethnopharmacol*. 2022;292:115213. doi:10.1016/j.jep.2022.115213
38. Kwon OY, Ryu S, Choi JK, Lee SH. *Smilax glabra* Roxb. Inhibits Collagen Induced Adhesion and Migration of PC3 and LNCaP Prostate Cancer Cells through the Inhibition of Beta 1 Integrin Expression. *Molecules*. 2020;25(13):3006. doi:10.3390/molecules25133006
39. Guo Y, Mao W, Jin L, et al. Flavonoid Group of *Smilax glabra* Roxb. Regulates the Anti-Tumor Immune Response Through the STAT3/HIF-1 Signaling Pathway. *Front Pharmacol*. 2022;13:918975. doi:10.3389/fphar.2022.918975
40. Tian T, Wang Z, Zhang J. Pathomechanisms of Oxidative Stress in Inflammatory Bowel Disease and Potential Antioxidant Therapies. *Oxid Med Cell Longev*. 2017;2017:4535194. doi:10.1155/2017/4535194
41. Sies H. Oxidative stress: a concept in redox biology and medicine. *Redox Biol*. 2015;4:180–183. doi:10.1016/j.redox.2015.01.002
42. O'Neill S, Brault J, Stasia MJ, Knaus UG. Genetic disorders coupled to ROS deficiency. *Redox Biol*. 2015;6:135–156. doi:10.1016/j.redox.2015.07.009
43. Goyette P, Labbé C, Trinh TT, Xavier RJ, Rioux JD. Molecular pathogenesis of inflammatory bowel disease: genotypes, phenotypes and personalized medicine. *Ann Med*. 2007;39(3):177–199. doi:10.1080/07853890701197615
44. Xu C, Feng C, Huang P, et al. TNFα and IFNγ rapidly activate PI3K-AKT signaling to drive glycolysis that confers mesenchymal stem cells enhanced anti-inflammatory property. *Stem Cell Res Ther*. 2022;13(1):491. doi:10.1186/s13287-022-03178-3
45. Lu Y, Li X, Liu S, Zhang Y, Zhang D. Toll-like Receptors and Inflammatory Bowel Disease. *Front Immunol*. 2018;9:72. doi:10.3389/fimmu.2018.00072
46. Hu X, Qi C, Feng F, et al. Combining network pharmacology, RNA-seq, and metabolomics strategies to reveal the mechanism of Cimicifugae Rhizoma-*Smilax glabra* Roxb herb pair for the treatment of psoriasis. *Phytomedicine*. 2022;105:154384. doi:10.1016/j.phymed.2022.154384
47. Hall PA, Coates PJ, Ansari B, Hopwood D. Regulation of cell number in the mammalian gastrointestinal tract: the importance of apoptosis. *J Cell Sci*. 1994;107(Pt 12):3569–3577. doi:10.1242/jcs.107.12.3569
48. Zhang J, Cen L, Zhang X, et al. MPST deficiency promotes intestinal epithelial cell apoptosis and aggravates inflammatory bowel disease via AKT. *Redox Biol*. 2022;56:102469. doi:10.1016/j.redox.2022.102469

49. Hartl K, Bayram Ş, Wetzel A, et al. p53 terminates the regenerative fetal-like state after colitis-associated injury. *Sci Adv*. 2024;10(43):eadp8783. doi:10.1126/sciadv.adp8783
50. Chang WC, Coudry RA, Clapper ML, et al. Loss of p53 enhances the induction of colitis-associated neoplasia by dextran sulfate sodium. *Carcinogenesis*. 2007;28(11):2375–2381. doi:10.1093/carcin/bgm134
51. Baliakas P, Soussi T. The TP53 tumor suppressor gene: from molecular biology to clinical investigations. *J Intern Med*. 2025;298(2):78–96. doi:10.1111/joim.20106
52. Yoshida T, Mikami T, Mitomi H, Okayasu I. Diverse p53 alterations in ulcerative colitis-associated low-grade dysplasia: full-length gene sequencing in microdissected single crypts. *J Pathol*. 2003;199(2):166–175. doi:10.1002/path.1264
53. Yin J, Harpaz N, Tong Y, et al. p53 point mutations in dysplastic and cancerous ulcerative colitis lesions. *Gastroenterology*. 1993;104(6):1633–1639. doi:10.1016/0016-5085(93)90639-T
54. Petitjean A, Achatz MI, Borresen-Dale AL, Hainaut P, Olivier M. TP53 mutations in human cancers: functional selection and impact on cancer prognosis and outcomes. *Oncogene*. 2007;26(15):2157–2165. doi:10.1038/sj.onc.1210302
55. Vermeulen L, Morrissey E, van der Heijden M, et al. Defining stem cell dynamics in models of intestinal tumor initiation. *Science*. 2013;342(6161):995–998. doi:10.1126/science.1243148

Clinical and Experimental Gastroenterology

Dovepress
Taylor & Francis Group

Publish your work in this journal

Clinical and Experimental Gastroenterology is an international, peer-reviewed, open access, online journal publishing original research, reports, editorials, reviews and commentaries on all aspects of gastroenterology in the clinic and laboratory. This journal is indexed on American Chemical Society's Chemical Abstracts Service (CAS). The manuscript management system is completely online and includes a very quick and fair peer-review system, which is all easy to use. Visit http://www.dovepress.com/testimonials.php to read real quotes from published authors.

Submit your manuscript here: https://www.dovepress.com/clinical-and-experimental-gastroenterology-journal